hsa_circ_0000231 promotes colorectal cancer cell growth through upregulation of CCND2 by IGF2BP3/miR-375 dual pathway

Wei Zhang
Peking University People's Hospital https://orcid.org/0000-0002-2001-1052
Bo Wang
Peking University People's Hospital
Yang Yang
Peking University People's Hospital
Zhen Zhang
Peking University People's Hospital
Quan Wang
Peking University People's Hospital
Haoran Zhang
Peking University People's Hospital
Kewei Jiang
Peking University People's Hospital
Yingjiang Ye
Peking University People's Hospital
Shan Wang
Peking University People's Hospital
Zhanlong Shen (shenlong1977@163.com)

Research

Keywords: Colorectal Cancer, circRNA, IGF2BP3, miR-375, CCND2

Posted Date: August 20th, 2020

DOI: https://doi.org/10.21203/rs.3.rs-47893/v2

Abstract

Background and aim Circular RNAs (circRNAs) have emerged as vital regulators of the initiation and progression of diverse kinds of human cancers. This study aimed to investigate the role of circRNAs in colorectal cancer (CRC).

Methods The expression profiles of circRNAs in five pairs of CRC tissues and adjacent normal tissues were analyzed using microarray. Quantitative real-time polymerase chain reaction, *in situ* hybridization, and BaseScope Assay were used to determine the level and prognostic values of hsa_circ_0000231. Then, *in vitro* and *in vivo* functional experiments were performed to investigate the effects of hsa_circ_0000231 on cell proliferation. Mechanistically, fluorescence *in situ* hybridization, dual-luciferase reporter assay, and RNA pull-down and RNA immunoprecipitation experiments were performed to confirm the interaction between hsa_circ_0000231 and Insulin-like growth factor 2 mRNA-binding protein 3(IGF2BP3) or has_miR-375.

Results The expression of hsa_circ_0000231 was upregulated in CRC primary tissues, which indicated poor prognosis of patients with CRC. The results demonstrated that hsa_circ_0000231 could promote CRC cell proliferation as well as tumorigenesis *in vitro* and *in vivo*. The mechanistic analysis showed that hsa_circ_0000231 might, on the one hand, act as a competing endogenous RNA of miR-375 to promote cyclin D2 (CCND2) and, on the other hand, bind to the IGF2BP3 protein to prevent CCND2 degradation.

Conclusion The findings suggested that hsa_circ_0000231 facilitated CRC progression by sponging miR-375 or binding to IGF2BP3 to modulate CCND2, implying that has_circ_0000231 might be a potential new diagnostic and therapeutic biomarker of CRC.

Background

Colorectal cancer (CRC) is the third most commonly diagnosed cancer in men and the fourth most commonly diagnosed cancer in women worldwide[1]. The annual new cases of CRC account for its third place among malignant tumors, and the related deaths account for the fourth place[2]. CRC was the fifth most commonly diagnosed cancer and the fifth most common cause of death by cancer in China in 2014, with an age-standardized incidence rate of 17.52 per 100,000 and age-standardized mortality rate of 7.91 per 100 000[3].

CRC has become a major disease seriously threatening human health and posing a huge social and economic burden[4]. The treatment of CRC mainly adopts a comprehensive treatment mode centered on surgery, but the curative effect is still unsatisfactory. The molecular mechanism underlying the development of CRC is not completely clear, which is one of the important reasons for its high incidence and poor prognosis[5]. Recent studies have shown the importance of a new family of noncoding RNAs, circular RNAs (circRNAs), in the molecular regulation of tumorigenesis and progression. They have a covalently closed circular structure at the 3'-untranslated region (UTR) and 5'-UTR, are widely and

diversely present in eukaryotic cells, and have an endogenous RNA molecule that regulates gene expression[6-9]. The circRNA functions mainly via the endogenous RNA (ceRNA) mechanism, that is, circRNA acts as a "molecular sponge" and competitively binds to microRNA (miRNA) through an miRNA response element (MRE) to inhibit miRNA function. MiRNAs degrade or inhibit the expression of target genes through the RNA-induced silencing complex (RISC), which relies on the Argonaute2 (AGO2) protein[10].

MicroRNAs (miRNAs) are small noncoding RNAs with a size of 18–25 nucleotides, which function as post-transcriptional regulators of target mRNAs[11]. The increase in the expression of oncogenic miRNAs in cancer leads to the downregulation of tumor-suppressive genes. In contrast, the decrease in the expression of tumor-suppressive miRNAs enhances the expression of oncogenes. The findings indicated that miRNAs participated in the tumorigenesis and progression of various cancers, including colorectal cancer[12-14]. However, the upstream regulators of miRNAs are poorly understood. Pandolf et al. presented a theory called the competing endogenous RNA (ceRNA) hypothesis stating that lncRNAs, mRNAs, and pseudogenes could communicate with, and regulate, each other by competitively binding to the MREs, which provides a new mechanism of gene regulation[15]. A circRNA could also serve as a ceRNA to sequester away an miRNA from its target genes[16, 17]. Also, circRNAs could bind to RNA-protective proteins[18]. However, the biological functions of most circRNAs in the pathogenesis and progression of CRC and the underlying mechanisms remain largely unclear.

The present study found 425 significantly differentially expressed circRNAs in CRC tissues. The has_circ_0000231 upregulation was further discovered to sponge miR-375 and IGF2BP3 and hence regulate CRC progression. The hsa_circ_0000231 is vital in the development of CRC and participates in the molecular regulation of CRC by regulating the cell cycle.

Methods

Ethics statement

This study was conducted in accordance with the ethical standards, the Declaration of Helsinki, and national and international guidelines, and was approved by the authors' institutional review board, which adheres to generally accepted international guidelines for animal experimentation.

CircRNA microarray

Five pairs of CRC tumor tissues and corresponding adjacent noncancerous tissues were used for circRNA microarrays. The specimens were obtained from patients undergoing surgery in the Peking University People's Hospital in 2014; detailed information is shown in Additional file 1: Table S1.

Patients and samples

160 CRC patients who were diagnosed and underwent surgery in Peking University People's Hospital between 2014 and 2017 were included in this study. Fresh colorectal tumor tissues and matched normal colorectal mucosa tissues were obtained from all the 160 patients. The specimens were obtained and immediately frozen in liquid nitrogen and stored at −80 °C until RNA or protein extraction.

Cellular fluorescence *in situ* hybridization

The cells were fixed with 4% paraformaldehyde for 15 min and washed with phosphate-buffered saline (PBS) three times for 5 min each time. Further, they were permeabilized with 0.5% Triton X-100 at room temperature for 20 min and washed with PBS three times for 3 min each time. Then, pepsin freshly diluted with 3% citric acid was added and digested at room temperature for 15 min. Subsequently, the nucleic acid fragment was exposed, rinsed with PBS, mixed with 20 μL of a pre-hybrid solution, and pre-hybridized at 50°C for 2–4 h. The hsa_circ_0000231 or miR375-specific probe hybridized at a constant temperature of 50°C. Hybridization was carried out using SSC at 37°C, biotinylated mouse anti-digoxigenin was added dropwise, the fragment was washed with PBS three times for 3 min each time, and the excess solution was absorbed with the absorbent paper. After adding DAPI stain for 10 min, the specimen was subjected to nuclear staining and washed three times with PBS for 3 min each time; the excess solution was absorbed by the absorbent paper. The specimen was sealed with a liquid containing a fluorescent quencher, and the image was observed under a fluorescence microscope.

BaseScope assay

BaseScope assay was performed following the manufacturer's protocols (Advanced Cell Diagnostics, CA, USA). The tissues were sectioned at 5-μm thickness, placed onto Superfrost Plus slides (Fisher Scientific, Loughborough, UK), and allowed to dry overnight at 25°C. The sections were then baked at 60°C for 1 h before deparaffinized in xylene (twice for 5 min) and ethanol (twice for 2 min), and then dried by baking at 60°C for 2 min. Subsequently, hydrogen peroxide was applied for 10 min at 25°C, target retrieval was performed for 15 min at 100°C, and RNAscope Protease III was applied at 40°C for 30 min. The samples were rinsed twice in distilled water between treatments. BaseScope probes (Mm-1700024F13Rik, cat#709881) with positive controls (Hs-PPIB, cat # 701031; DapB, cat # 701011) were then applied, and the samples were incubated for 2 h at 40°C in a HybEZ oven and then with reagents AMP0 (30 min at 40°C), AMP1 (15 min at 40°C), AMP2 (30 min at 40°C), AMP3 (30 min at 40°C), AMP4 (15 min at 40°C), AMP5 (30 min at 25°C), and AMP6 (15 min at 25°C). The slides were rinsed with wash buffer (twice for 2 min) between AMP incubation steps. Finally, they were treated with Fast Red for 10 min at 25°C in the dark, counterstained with Gill's hematoxylin, dried for 15 min at 60°C, and mounted in Catamount permanent mounting medium (Vector Labs, CA, USA).

RNA extraction and quantitative real-time polymerase chain reaction

Total RNA from cell lines and tissue samples was extracted using TRIzol (Invitrogen, USA) following the manufacturer's instructions. For the plasma, the total RNAs were extracted using an mirVana PARISTM microRNA extraction kit (ABI, USA) following the manufacturer's protocols. For lncRNA quantification,

GAPDH was used as internal control, and PrimeScript RT Master Mix (QIAGEN, Germany) was used for reverse transcription and real-time polymerase chain reaction (PCR). The primer sequences are listed in Additional file 1: Table S2. All reactions were performed in triplicate. The fold change for each gene relative to the control group was calculated using the $2^{-\Delta\Delta Ct}$ method.

Lentiviral short hairpin RNA particles

Recombinant lentiviral particles expressing hsa_circ_0000231 or hsa_circ_0000231 small interfering (si) RNA were obtained from GenePharm Co., Ltd. (Shanghai, China). SW480 cells were grown to approximately 40% confluence and infected with lentiviral particles in complete medium for 48 h. They were co-treated with the cationic polymer polybrene (8 g/mL in water) to increase the infection efficiency. Neither shRNA nor polybrene affected cell viability. Further, siRNA and shRNA had no off-target effects, and did not affect cell adherence, shape, or viability at the indicated multiplicity of infection.

Cell transfection

For *in vitro* studies, siRNA interference sequences targeting hsa_circ_0000231 were designed and synthesized (Ribobio, Guangzhou, China) to interfere with the expression of hsa_circ_0000231, and a final concentration of 50nM was used for transient transfection. Full-length human hsa_circ_0000231 cDNA was cloned into the pcDNA3.1 expression vector (Genechem, Shanghai, China) to overexpress hsa_circ_0000231. Lipofectamine 3000 (Invitrogen, CA, USA) was used for transfection following the manufacturer's protocols.

For *in vivo* assays, the hsa_circ_0000231 overexpression cell line was used. The hsa_circ_0000231 gene was cloned into a lentivirus vector LV-GFP-Puro, and SW480 cells were used for infection. Stable transfection cells were established by puromycin antibiotic selection for 7 days, with a concentration of 2.5 μg/mL. The hsa_circ_0000231-overexpressing cells and control cells were named SW480-LV-hsa_circ_0000231 and SW480-LV-NC, respectively.

Transfection and grouping of cells: Cell transfection were performed in strict accordance with the instructions of Invitrogen's Lipofectamine 3000 Transfection Reagent when the cytoplasm was inoculated with a confluence of about 80%. The Lipofectamine 3000 reagent was diluted with OPTI-MEM culture medium and mixed. The DNA expression plasmid to be transfected was diluted with OPTI-MEM culture medium and mixed with P3000 reagent. The diluted DNA expression plasmid was added in equal volume to each dilution of Lipofectamine 3000 reagent and incubated at room temperature for 5 min. The DNA–liposome mixture was added to the cell suspension and carefully mixed. The culture was continued in a 5% CO_2 incubator at 37°C.

Cell proliferation assay

SW480 and SW620 cells (3×10^3 cells) were seeded in complete medium in 96-well plates and infected with hsa_circ_0000231 siRNA. The cell proliferation assay was performed with a Cell Counting Kit 8

(CCK8) following the manufacturer's protocol, and cell proliferation was detected after 0, 24, 48, 72, and 96 h. The cells in each group were tested for five replicates. The cell proliferation was evaluated by the CCK-8 method using a microplate reader (Molecular Devices, CA, USA) following the manufacturer's protocols to measure the absorbance.

For the colony formation assay, the transfected cells were seeded into each well of a six-well plate on day 0 and then incubated for another 14 days. Then, the wells were fixed with 4% paraformaldehyde and stained with 0.1% crystal violet. The colonies so formed were counted and analyzed using Image J software.

CCK-8 method for detecting cell proliferation curve

The proliferation of CRC cells in each group was detected using the CCK-8 method. After transfection for 24 h, the cells were seeded in 96-well plates at 5×10^3 cells/well, and 10 μL of CCK-8 solution was added to each well. Then, the cells were incubated in a 5% CO_2 incubator at 37°C. After the cells were grown for 2, 3, 4, and 5 days, the absorbance of the cells at 450 nm was measured using an enzyme reader to represent the proliferative activity of the cells during this period. The proliferation curve of each group of cells was plotted, and the difference in the cell proliferation rate was compared between the groups.

Western blot analysis

The cells were lysed in RIPA buffer and centrifuged at high speed, followed by protein quantification using a bicinchoninic acid assay. The cellular proteins were separated by sodium dodecyl sulfate–polyacrylamide gel electrophoresis (SDS-PAGE) and transferred onto polyvinylidene difluoride (PVDF) membranes. The membranes were incubated with primary antibodies, followed by a horseradish peroxidase (HRP)-labeled secondary antibody. GAPDH was used as a loading control. The total protein of CRC cells was diluted with RIPA buffer, separated using 10% SDS-PAGE, and then electrotransferred onto a PVDF membrane (Bio-Rad, CA, USA). The membranes were blocked with 5% skimmed milk powder and incubated with primary antibodies against CCND2 (1:1000), IGF2BP3 (1:1000) (Abcam, CA, USA), RB (1:500), and GAPDH (1:5000) (Cell Signaling Technology, MA, USA) at 4°C overnight and then incubated with secondary antibodies (1:5000) (Cell Signaling Technology, MA, USA) at room temperature for 2 h. Finally, the bands were examined by an Immobilob Western Chemiluminescent HRP Substrate (Millipore, MA, USA). The antibodies used in the experiments are shown in Additional file 1: Table S3.

Luciferase reporter assay

The hsa_circ_0000231 and CCND2 fragments containing two putative wild-type or mutated miR-375-binding sites were amplified by PCR and cloned downstream of the luciferase gene in the pGL3 vector (Promega, WI, USA). The constructed reporter vectors were verified by sequencing. Luciferase reporter assays were performed by transiently co-transfecting HEK293T cells in 24-well plates with the reporter vectors, miR-216a, and the Renilla luciferase construct using Lipofectamine 2000 (Invitrogen, MA, USA).

After 48-h transfection, the cells were harvested, and luciferase activity was measured using a dual-luciferase reporter assay system (Promega) and normalized to that of Renilla luciferase.

Biotin-labeled RNA pull-down and mass spectrometry analysis

Biotin-labeled RNA for the linear sequence of has_circ_0000231 and CCND2 was generated by an *in vitro* transcription reaction with the Biotin RNA Labeling Mix (Roche, Mannheim, Germany) and T7 RNA polymerase (Roche), and then treated with RNase-free DNase I (TaKaRa, Japan). After incubation with the oligonucleotide targeting circular junction, the liner probe was circularized using T4 RNA ligase I and treated with RNase R. After purification with a RNeasy Mini Kit (Qiagen, Inc., CA, USA), the biotin-labeled RNA probe (3 μg) was incubated with cell extracts from CRC cells at room temperature for 2 h and treated with 35 μL of Streptavidin C1 magnetic beads (Invitrogen) for 1 h. After washing, the retrieved protein was detected by Western blot or mass spectrometry analysis (CapitalBio Technology, Beijing, China).

RNA immunoprecipitation

RNA immunoprecipitation (RIP) was conducted with a Magna RIP kit (Millipore, MA, USA) following the manufacturer's instructions. SW480 cells were harvested 48 h after the transfection of miR-375 mimics or miR-NC and lysed in complete RNA lysis buffer. The cell lysates were incubated with magnetic beads conjugated with anti-AGO2 (Millipore) or negative control immunoglobulin antibody (Millipore) at 4°C for 4 h. The beads were washed with wash buffer. Then, immunoprecipitated RNA and protein were purified and enriched to detect the target RNAs and AGO2 using qRT-PCR and Western blot analysis.

Nude mouse model of ectopic tumors

BALB/c nude (nu/nu) mice, aged 6 weeks old were purchased from Beijing Weitong Lihua Experimental Animal Technology Co., Ltd. Tumors were generated by the subcutaneous injection of 2×10^6 SW480 cells infected with hsa_circ_0000231-overexpressing cells or control lentivirus particles and suspended in 50 L of PBS into the dorsal region near the thigh. Five mice were included in each group. The mice were then weighed and assessed for tumor size every 7 weeks by measuring the tumor length and width.

Statistical analysis

The data generated in this study were all analyzed using SPSS22.0 statistical software. The measurement data were expressed as mean ± standard deviation (x ± s). The two groups were compared using the *t* test for statistical analysis. The count data were analyzed using the χ^2 test. The survival rates were evaluated using the Kaplan–Meier method and tested using the log-rank test. The effects of clinical variables on the overall survival of patients with CRC were determined by univariate and multivariate Cox proportional hazards regression models. Age, T stage, N stage, clinical stage of distant metastasis, and expression of has_circ_0000231 were adjusted for variable analysis in the multivariate Cox proportional hazards regression model. The correlation between groups was analyzed by Pearson correlation, and a *P* value <0.05 was used as a criterion for statistically significant differences.

Results

Expression of hsa_circ_0000231 was upregulated in CRC specimens and associated with the progression and poor prognosis of patients with CRC

Arraystar circular RNA chip experiments were conducted in paired CRC tissues and para-cancerous tissues from five patients with CRC to understand the expression profiles of circRNA in CRC. With a cutoff criteria of fold change >1.5 and P <0.05, 425 circRNAs were found to be differentially expressed, of which 278 were upregulated and 147 were downregulated (Fig. 1A and 1B). Besides, the exon-related circRNAs were the maximum according to the classification analysis of circRNAs (Fig. 1C Additional file 1: Table S4). Further, hsa_circ_0000231 was the most upregulated (4.557-folds) circRNA, which was spliced from ARHGAP12 located at chr10:32197099-32199491 and finally formed a circular transcript of 794 nucleotides according to the annotation of circBase (http://www.circbase.org/).

A randomized selection of 10 circRNAs with significant differential expression in 10 pairs of CRC tissues showed quantitative PCR detection, and the results were consistent with the chip results, indicating that the chip analysis results were credible (Fig. 1D). Further quantitative PCR was performed to detect the expression of hsa_circ_0000231 in nine CRC cell lines, including SW480, SW620, LoVo, HT29, HCT116, RKO, LS174T, COLO-215, and HCT8, along with human normal colorectal epithelial cell–derived NCM460 cells. The results showed that has_circ_0000231 was detected in the aforementioned cell lines. Also, their expression level in cancer cell lines was higher than that in NCM460 cells (Fig. 1E).

The expression of hsa_circ_0000231 in colon cancer tissues and adjacent normal tissues in 160 patients was detected by quantitative PCR. The results showed that the expression of hsa_circ_0000231 was higher in tumor tissues than in adjacent normal tissues by 1.39 times (Fig. 1F).

The statistical analysis of the expression of hsa_circ_0000231 in CRC tissues and the clinical pathological parameters of patients revealed that the expression level of hsa_circ_0000231 correlated with tumor size, depth of invasion, and TNM stage of patients (Table 1). A survival analysis was conducted to determine the relationship of hsa_circ_0000231 with overall survival (OS) and disease-free survival (DFS) in patients with CRC. Patients with high expression of hsa_circ_0000231 in CRC had significantly shorter OS and lower DFS, with statistically significant differences (Fig. 1G and 1H). Further univariate and multivariate Cox regression analyses showed that TNM stage and hsa_circ_0000231 expression levels were independent prognostic factors for patients with CRC (Table S5).

Has_circ_0000231 promoted CRC cell proliferation and modulated cell cycle and colony formation but with no apoptosis

The effect of hsa_circ_0000231 on cell proliferation was detected using the CCK-8 assay. The proliferation ability was significantly weakened in SW480 cells or SW620 cells in the has_circ_0000231 siRNA and hsa_circ_0000231 combined with si-mRNA groups compared with the control group (P < 0.05) (Fig. 2A and 2B).

The flow cytometry analysis with Annexin V/PI double staining showed no significant difference in the apoptotic rate of SW480 and SW620 cells transfected with each group of siRNAs in the si-circ_0000231 group compared with the negative control (si-NC) group (Fig. 2C and 2D).

After transfection with siRNAs in each group, no significant difference was observed in the apoptotic rate of SW480 cells and SW620 cells between the si-mRNA, si-circ_0000231 and the si-both groups compared with the negative control group (si-NC) (Fig. 2E and 2F).

The cell cycle detection by flow cytometry revealed that the percentage of G0/G1 cells obviously increased after inhibiting the expression of hsa_circ_0000231 in SW480 and SW620 cells. These results indicated that the knockdown of hsa_circ_0000231 induced G0/G1 phase arrest in CRC cell lines (Fig. 2G and 2H).

Hsa_circ_0000231 facilitated the tumorigenesis and proliferation of CRC cells *in vivo*

SW480 cells were stably transfected with the overexpression or mock vector, infected with lentivirus negative control (LV-NC) or LV-circ, and then subcutaneously injected into female nude mice to determine the effects of hsa_circ_0000231 on tumor growth *in vivo*. The tumors derived from cells overexpressing hsa_circ_0000231 were bigger and heavier than those in the control group (Fig. 2I–2K). These results confirmed the oncogenic role of hsa_circ_0000231 in the development of CRC, suggesting the involvement of hsa_circ_0000231 in the progression of CRC.

CCND2 might be a downstream target of has_circ_0000231 in CRC

A specific siRNA was used to interfere with hsa_circ_0000231 so as to further clarify how hsa_circ0000231 functioned in CRC, given that hsa_circ0000231 affected the CRC cell cycle process. The PCR chip (Cell Cycle PCR array, Qiagen) testing of cell cycle–related genes found that the expression of 18 genes of the 84-cell cycle–related genes more than doubled compared with the control group. The 10 genes with the most decreased expression are depicted in Figure S1A. The downregulation of CCND2, CCND1, CDK6, CDKN3, and CCND2 was the most obvious (the downregulation factor was more than three times). The qPCR experiment verified that the mRNA expression trends of CCND2, CCND1, CDK6, CDKN3, and CCND2 were consistent with the cell cycle chip results, and their expression was downregulated (Fig. S1B). CCND2 was found to be the most upregulated cell cycle–related gene in CRC tissues. The cell cycle can act as a convergence point for oncogenic signaling pathways, and aberrant cell cycle progression is a crucial characteristic of cancers. Hence, the present study focused on hsa_circ_0000231 and CCND2 in the tumorigenesis and progression of CRC.

The qRT-PCR was used to detect CCND2, and the expression was found to be significantly reduced after interference with hsa_circ_0000231 (Fig. S1C). Then, the expression of CCND2 in 160 CRC cohorts was detected by qPCR. The results showed that the expression of CCND2 was notably higher in tumor tissues than in adjacent normal tissues (Fig. S1D). The survival analysis was performed to reveal that patients with high expression of CCND2 had significantly shorter OS (Fig. S1E). Besides, the expression of CCND2

positively correlated with has_circ_0000231 (Fig. S1F). Also, the expression of CCND2 correlated with tumor size and TNM stage (Table 1). In a study on nude mice, the Western blot analysis revealed that the expression of CCND2 in hsa_circ_0000231-overexpressing tumor tissues was much higher than that in the mock group (Fig. S1G and S1H).

Hsa_circ_0000231 functioned as a sponge for miR-375

The potential targets of hsa_circ_0000231 were predicted using miRNA target prediction software made by Arraystar according to the TargetScan and miRanda database to elucidate the molecular mechanism underlying hsa_circ_0000231 regulating CCND2, given that circRNAs might act as a sponge for microRNAs further modulating downstream targets. The results showed that hsa_circ_0000231 possessed a conserved target site of miR-375 with a high score (Fig. 3A). Considering that circRNAs could serve as miRNA sponges in the cytoplasm, fluorescence *in situ* hybridization and BaseScope Assay were performed in CRC cells and tissues to observe the subcellular localization of hsa_circ_0000231. Most of hsa_circ_0000231 was located in the cytoplasm (Fig. 3B and 3C). Then, the levels of miR-375 were examined in 160 pairs of CRC tissues and adjacent noncancerous tissues. The results indicated that the expression of miR-375 was markedly downregulated in CRC tissues compared with adjacent nontumor tissues (Fig. 3D), and the expression of miR-375 negatively correlated with has_circ_0000231 (Figure 3E). Therefore, it was supposed that hsa_circ_0000231 might serve as a competing endogenous RNA (ceRNA) for miR-375.

The dual-luciferase reporter assay was applied in SW480 cells to confirm the bioinformatics prediction analysis. The full-length hsa_circ_0000231-WT and mutant version without miR-375-binding sites were subcloned into luciferase reporter vector psiCHECK2 (Fig. 3F). The results indicated that miR-375 mimics could significantly decrease the luciferase activity in the WT group but in the not mutant one (Fig. 3G), suggesting a direct interaction between hsa_circ_0000231 and miR-375.

MiRNAs regulate target gene expression by binding to AGO2, the key component of RISC. Therefore, an anti-AGO2 RIP assay was conducted in SW480 cells to pull down the RNA transcripts that bound AGO2 to the anti-AGO2 antibody, and IgG was used as a negative control. Indeed, AGO2, hsa_circ_0000231 and miR-375 were all efficiently pulled down by anti-AGO2 antibodies compared with IgG. Moreover, both hsa_circ_0000231 and miR-375 were significantly enriched in cells transfected with miR-375 mimics compared with the miR-NC group (Fig. 3H and 3I).

A circRNA pull-down assay with specific biotin-labeled hsa_circ_0000231 probes were performed to further verify the binding effect of hsa_circ_0000231 and miR-375. A specific enrichment of hsa_circ_0000231 and miR-375 was detected by qRT-PCR in the hsa_circ_0000231 probe group compared with the control probe group (Fig. 3J and 3K).

MiR-375 suppressed the growth of CRC cells *in vitro* and *in vivo*

The mimics-NC and miR-375 mimics were transfected into SW480 and SW620 cells, respectively, to explore the role of miR-375 in CRC cells. A CCK-8 assay was performed to detect the effect of miR-375 on cell proliferation. The results showed that the proliferation ability markedly decreased in the miR-375 mimics group and in SW480 cells or SW620 cells compared with the control group ($P < 0.05$) (Fig. S2A and S2B). The cell cycle detection by flow cytometry revealed that the percentage of G0/G1 cells obviously increased after the overexpression of miR-375 in SW480 and SW620 cells (Fig. S2C and S2D).

CCND2 was directly targeted by miR-375 and indirectly regulated by hsa_circ_0000231

According to the TargetScan (http://www.targetscan.org), CCND2 and hsa_circ_0000231 shared the same MRE of miR-375 (Fig. 4A). The present study found that miR-375 mimics could markedly reduce the expression of CCND2, while miR-375 inhibitors significantly enhanced the level of CCND2 in SW480 cells. The increase or decrease in CCND2 expression induced by miR-375 mimics or inhibitors could be markedly reversed by hsa_circ_0000231 overexpression or knockdown, respectively, in SW480 cells, as detected by qPCR and Western blot analysis (Fig. 4B–4D). These data suggested that hsa_circ_0000231 could regulate the expression of CCND2 by serving as a ceRNA for miR-375 in CRC.

The dual-luciferase reporter assay was conducted to validate the aforementioned prediction. The results showed that the activity of luciferase reporter vector carrying the CCND2 3’-UTR-WT sequence was significantly decreased by miR-375 mimics compared with the miR-NC groups (Fig. 4E and 4F). Moreover, the luciferase activity was recovered after transfection with hsa_circ_0000231 in the miR-375 + CCND2 3’-UTR-WT group (Fig. 4G). Furthermore, an anti-AGO2 RIP assay was performed to detect the relationship between miR-375 and CCND2. The result showed that miR-375 pull-down by CCND2 was specifically enriched in SW480 cells (Fig. 4H and 4I). Then, an RNA pull-down assay was performed in SW480 cells. The analysis demonstrated that endogenous CCND2 was significantly pulled down by biotinylated probes against miR-375 (Fig. 4J and 4K).

IGF2BP3 could bind to has_circ_0000231 and CCND2, as an RBP to prevent RNA degradation

The circBase and Circular RNA interactome databases were used to predict RNA-binding proteins (RBP) that could bind to hsa_circ_0000231. IGF2BP3 had a binding site with hsa_circ_0000231, and it could be perfectly matched to the 3'-UTR region of the CCND2 gene mRNA, which was also the seed sequence region of miR375. An anti-IGF2BP3 RIP assay was performed to detect the expression of hsa_circ_0000231 and CCND2 so as to verify the combination of IGF2BP3 with hsa_circ_0000231 and CCND2. The result showed that both hsa_circ_0000231 and CCND2 were significantly enriched in SW480 and SW620 cells (Fig. 5A and 5B). Still, an RNA pull-down assay was conducted in SW480 and SW620 cell lines. The analysis demonstrated that IGF2BP3 was remarkably pulled down by biotinylated probes against both has_circ_0000231 and CCND2 (Fig. 5C and 5D).

IGF2BP3 was overexpressed to confirm that it exerted a protective effect by increasing the expression of hsa_circ_0000231 and CCND2 in CRC cells. The overexpression of IGF2BP3 could markedly enhance the expressions of hsa_circ_0000231 and CCND2 in SW480 and SW620 cells (Fig. 5E and 5F). These data

suggested that IGF2BP3 might increase the expression of CCND2 through RBP binding to both hsa_circ_0000231 and CCND2 in CRC. Moreover, Western blot analysis was conducted to confirm that the upregulation or downregulation of IGF2BP3 markedly enhanced or decreased the expression of CCND2, and the effect of IGF2BP3 could be partially reversed by mimics or inhibitor of miR-375 in SW480 and SW620 cells (Fig. 5G–5J).

Hsa_circ_0000231 promoted CRC proliferation through the hsa_circ_0000231/IGF2BP3/miR-375/CCND2 axis

Rescue experiments were applied using miR-375 mimics and inhibitors to ensure whether hsa_circ_0000231 executed its biological function through the hsa_circ_0000231/IGF2BP3/miR-375/CCND2 axis. The results indicated that the miR-375 mimics reversed the proliferation-promoting effects of hsa_circ_0000231 overexpression in SW480 cells, whereas miR-375 inhibitors could rescue the proliferation-suppressing effects of the knockdown of hsa_circ_0000231 in SW620 cells, as detected by the CCK8 assay. The effects caused by an increase or decrease in the expression of hsa_circ_0000231 could be partially rescued by si-IGF2BP3 or overexpression of IGF2BP3 in SW480 and SW620 cells, respectively (Fig. 6A and 6B). In summary, these data demonstrated that hsa_circ_0000231 might serve as a ceRNA for miR-375 and was protected by IGF2BP3 to regulate CCND2 expression, leading to uncontrolled cell cycle and development of CRC (Fig. 6C).

Discussion

The circRNA is abnormally expressed in various cancers, such as esophageal cancer[19], gastric cancer[20], pancreatic cancer[21], breast cancer[22]and liver cancer[23], It is associated with cell proliferation, invasion, and metastasis, and even patient prognosis. The reports on the role of circRNA in CRC are mostly related to the relationship between circRNA and clinicopathological indicators; a few in-depth studies were performed on molecular regulation mechanisms. Circ0000069 promotes the proliferation, invasion, and migration of CRC cells and is associated with age, lymph node metastasis, and TNM staging in patients with CRC[24]. However, the molecular mechanism by which circular RNA regulates target gene expression via molecular sponge action in CRC is not fully understood. The present study showed the overexpression of circ_0000231 in CRC tissues and cell lines, indicating the poor prognosis of patients with CRC. Furthermore, the multivariate analysis showed that the high expression of has_circ_0000231 and TNM stage were two independent prognostic factors for poor survival in patients with CRC.

The ceRNA hypothesis suggested that RNA transcripts, including mRNAs, lncRNAs, pseudogenes, and circRNAs, could crosstalk with, and regulate the expression of, each other via competing for shared MREs, building a new complicated post-transcriptional regulatory network and mechanism[15]. Increasing evidence indicated that some circRNAs could serve as sponges for miRNAs to regulate the expression of miRNA target genes in multiple human diseases[25], including colorectal cancer. For example, hsa_circ_001680 promoted CRC development by functioning as a sponge for miR-340 to influence the expression of BMI1[26]. Thus, fully understanding how has_circ_0000231 functioned in CRC would provide

a novel insight into the oncogenesis mechanism. The present study found using bioinformatics analysis that hsa_circ_0000231 contained the MRE of miR-375. Hsa_circ_0000231 and miR-375 were co-located in the cytoplasm of CRC cells and tissues. Further, the dual-luciferase reporter, anti-AGO2 RNA immunoprecipitation, and RNA pull-down assays confirmed that has_circ_0000231 could interact with miR-375 directly, indicating that circ_0000231 exerted an oncogenic effect via sponging miR-375 in CRC. Consistent with the results of the present study, miR-375 was significantly downregulated in CRC tissues and cell lines and negatively correlated with the degree of malignancy of CRC[27]. The findings of this study indicated that has_circ_0000231 served as an oncogene by sponging miR-375 in CRC, revealing the significance of interaction between has_circ_0000231, and miR-375 in the tumorigenesis and development of CRC.

According to the ceRNA hypothesis, circRNA could act as a ceRNA to modulate the expression of miRNA target genes. CCND2, a vital cell cycle regulator, and has_circ_0000231 were co-overexpressed in CRC, further confirming that the cell cycle was closely related to the tumorigenesis and development of CRC[28]. Moreover, the bioinformatics analysis indicated using miRcode and TargetScan that CCND2 was one of the potential targets of miR-375. Next, a dual-luciferase reporter assay confirmed that miR-375 could directly target the 3'-UTR of CCND2. Additionally, the upregulation of miR-375 led to the knockdown of CCND2 at the mRNA and protein levels, whereas the downregulation of miR-375 had an opposite effect. CCND2 mainly regulates the cell cycle progression[29]. The downregulation of has_circ_0000231 resulted in G1/S-phase cell cycle arrest. CCND2 was involved in determining progression through checkpoints in G1/S and G2/M phases that dictated whether a cell could proceed with DNA replication and cell division. The data suggested that has_circ_0000231 knockdown might inhibit the expression of CCND2, leading to decreased activity and G1/S-phase cell cycle arrest. The dysregulation of CCND2 activity was implicated in multiple cancers, including CRC[30]. Also, the overexpression of CCND2 was related to poor prognosis in CRC[31].

Consistent with previous findings, the present study found that CCND2 was significantly regulated in CRC tissues and the overexpression of CCND2 correlated with shorter OS. This study showed that the overexpression of hsa_circ_0000231 could increase the expression of CCND2 at both mRNA and protein levels, while the knockdown of hsa_circ_0000231 exhibited a reverse effect, thus validating the crosstalk between hsa_circ_0000231 and CCND2. Furthermore, these effects could be partially abolished by miR-375 mimics or inhibitors, hence supporting the hypothesis that hsa_circ_0000231 functioned as a ceRNA to promote CCND2-mediated proliferation via decoying miR-375 in CRC.

Besides, RBP is vital in the regulation of post-transcriptional gene expression, and circRNA may act as an RBP "super sponge" by binding to RBP, thus changing the splicing pattern or mRNA stability. In the present study, a circular RNA interactome database was used to forecast that IGF2BP3 might combine with hsa_circ_0000231 via RBA-protein-binding sites. Another study found through http://starbase.sysu.edu.cn prediction that IGF2BP3 also combined with CCND2. IGF2BP3 is a member of the RBP family and functions in many biological processes, such as mRNA localization, translation, and stability

maintenance[32]. Previous studies found that the expression of IGF2BP3 was associated with the occurrence, metastasis, and poor prognosis of malignant tumors[33]. Regarding the regulatory effect of IGF2BP3 on target genes, some studies suggested that the IGF2BP3 protein bound to the 3'-UTR of target gene mRNA and compete with miRNA for binding sites, thus protecting the mRNA of target genes from miRNA degradation, including maintaining the stability of CCND2 mRNA and promoting CCND2 translation[34, 35].

Therefore, it was speculated that IGF2BP3 could enhance the stability of has_circ_0000231 and protect CCND2 from degradation via miR-375. To confirm a previous suggestion, it was presumed that IGF2BP3 might bind to has_circ_0000231 and CCND2 at the same time, and the binding site was consistent with the binding site of miR-375 and CCND2. RIP, RNA pull-down, qRT-PCR, and Western blot assays were further performed to confirm that the expression of hsa_circ_0091073 and CCND2 could be upregulated by increasing the expression of IGF2BP3, while the expression of hsa_circ_0091073 and CCND2 was downregulated by interfering with the expression of the *IGF2BP3* gene. Meanwhile, IGF2BP3 protected CCND2 from the regulation of miR-375, and the regulatory effect of miR-375 on CCND2 was opposite to that of IGF2BP3.vTherefore, IGF2BP3 might not only bind to has_circ_0000231 but also inhibit the degradation of CCND2 mRNA by miR-375 at the 3'-UTR binding site of CCDN2 mRNA, thus maintaining the stability of CCND2 mRNA.

Conclusions

In conclusion, the results suggested that increased hsa_circ_0000231 expression was a frequent event and a potential independent prognosis marker of CRC. This study was novel in demonstrating that hsa_circ_0000231 might sponge miR-375 to modulate CCND2 expression, and IGF2BP3 could protect hsa_circ_0000231 and CCND2, leading to the tumorigenesis and development of CRC. The findings suggested that has_circ_0000231 could be a valuable prognosis marker and a promising diagnostic and therapeutic target for CRC in the future. The regulatory network involving the hsa_circ_0000231/IGF2BP3/miR-375/CCND2 axis might provide a better understanding of the potential mechanism underlying the pathogenesis and progression of CRC.

Declarations

Ethics approval and consent to participate

This study was performed according to the recommendations in the Guide for the Chinese Ethics Review Committees. The protocol was approved by the Ethics Committee of Peking University People's Hospital. Written informed consent was obtained from each subject. The animal experiment was carried out under ethics approval of Peking University People's Hospital.

Consent for publication

All contributing authors agree to the publication of this article.

Availability of data and materials

All data are fully available without restriction.

Competing interests

The authors declare that they have no competing interests.

Funding

This work was funded by National Natural Science Foundation of China (81572383, 81672375, 81702354, 81871962, 81972240) and Beijing Municipal Natural Science Foundation (7182171)

Authors' contributions

WZ and ZLS conceived the study and participated in its design and coordination; ZW, BW and ZZ performed the experiments; HRZ and YY collected and analyzed the clinical data. QW, KWJ and SW analyzed and interpreted the data; WZ drafted the manuscript; BW and ZLS revised the manuscript; all authors read and approved the final manuscript.

Acknowledgements

We would like to thank MedSci for English language editing.

Authors' information

[1]Department of Gastroenterological Surgery, Peking University People's Hospital, Beijing 100044, PR China

[2]Laboratory of Surgical Oncology, Peking University People's Hospital, Beijing 100044, PR China

[3]Beijing Key Laboratory of Colorectal Cancer Diagnosis and Treatment Research, Peking University People's Hospital, Beijing 100044, PR China

Abbreviations

circRNA: circular RNA, CRC: colorectal cancer, ceRNA: competing endogenous RNA, CCND2: cyclin D2, MRE: miRNA response element, miRNA: microRNA, siRNA: small interfering RNA, RIP: RNA immunoprecipitation, AGO2: anti-Argonaute2, RBP: RNA binding protein

References

1. Dekker E, Tanis PJ, Vleugels JLA, Kasi PM, Wallace MB. Colorectal cancer. The Lancet 2019; 394:1467-80.

2. Siegel RL, Miller KD, Jemal A. Cancer statistics, 2020. CA: a cancer journal for clinicians 2020; 70:7-30.
3. Chen H, Li N, Ren J, Feng X, Lyu Z, Wei L, Li X, Guo L, Zheng Z, Zou S, Zhang Y, Li J, Zhang K, Chen W, Dai M, He J, Group OCSP. Participation and yield of a population-based colorectal cancer screening programme in China. GUT 2019; 68:1450-7.
4. Navarro M, Nicolas A, Ferrandez A, Lanas A. Colorectal cancer population screening programs worldwide in 2016: An update. World J Gastroenterol 2017; 23:3632-42.
5. Lai Y, Wang C, Civan JM, Palazzo JP, Ye Z, Hyslop T, Lin J, Myers RE, Li B, Jiang B, Sama A, Xing J, Yang H. Effects of Cancer Stage and Treatment Differences on Racial Disparities in Survival From Colon Cancer: A United States Population-Based Study. GASTROENTEROLOGY 2016; 150:1135-46.
6. Su M, Xiao Y, Ma J, Tang Y, Tian B, Zhang Y, Li X, Wu Z, Yang D, Zhou Y, Wang H, Liao Q, Wang W. Circular RNAs in Cancer: emerging functions in hallmarks, stemness, resistance and roles as potential biomarkers. MOL CANCER 2019; 18.
7. Shang Q, Yang Z, Jia R, Ge S. The novel roles of circRNAs in human cancer. MOL CANCER 2019; 18.
8. Naeli P, Pourhanifeh MH, Karimzadeh MR, Shabaninejad Z, Movahedpour A, Tarrahimofrad H, Mirzaei HR, Bafrani HH, Savardashtaki A, Mirzaei H, Hamblin MR. Circular RNAs and gastrointestinal cancers: Epigenetic regulators with a prognostic and therapeutic role. Critical Reviews in Oncology/Hematology 2020; 145:102854.
9. Naeli P, Pourhanifeh MH, Karimzadeh MR, Shabaninejad Z, Movahedpour A, Tarrahimofrad H, Mirzaei HR, Bafrani HH, Savardashtaki A, Mirzaei H, Hamblin MR. Circular RNAs and gastrointestinal cancers: Epigenetic regulators with a prognostic and therapeutic role. Critical Reviews in Oncology/Hematology 2020; 145:102854.
10. Kristensen LS, Andersen MS, Stagsted L, Ebbesen KK, Hansen TB, Kjems J. The biogenesis, biology and characterization of circular RNAs. NAT REV GENET 2019; 20:675-91.
11. Garzon R, Marcucci G, Croce CM. Targeting microRNAs in cancer: rationale, strategies and challenges. NAT REV DRUG DISCOV 2010; 9:775-89.
12. Sakaguchi M, Hisamori S, Oshima N, Sato F, Shimono Y, Sakai Y. miR-137 Regulates the Tumorigenicity of Colon Cancer Stem Cells through the Inhibition of DCLK1. MOL CANCER RES 2016; 14:354-62.
13. Lv C, Li F, Li X, Tian Y, Zhang Y, Sheng X, Song Y, Meng Q, Yuan S, Luan L, Andl T, Feng X, Jiao B, Xu M, Plikus MV, Dai X, Lengner C, Cui W, Ren F, Shuai J, Millar SE, Yu Z. MiR-31 promotes mammary stem cell expansion and breast tumorigenesis by suppressing Wnt signaling antagonists. NAT COMMUN 2017; 8:1036.
14. Panza E, Ercolano G, De Cicco P, Armogida C, Scognamiglio G, Botti G, Cirino G, Ianaro A. MicroRNA-143-3p inhibits growth and invasiveness of melanoma cells by targeting cyclooxygenase-2 and inversely correlates with malignant melanoma progression. BIOCHEM PHARMACOL 2018; 156:52-9.
15. Salmena L, Poliseno L, Tay Y, Kats L, Pandolfi PP. A ceRNA Hypothesis: The Rosetta Stone of a Hidden RNA Language? CELL 2011; 146:353-8.

16. Wu P, Mo Y, Peng M, Tang T, Zhong Y, Deng X, Xiong F, Guo C, Wu X, Li Y, Li X, Li G, Zeng Z, Xiong W. Emerging role of tumor-related functional peptides encoded by lncRNA and circRNA. MOL CANCER 2020; 19.
17. Zhong Y, Du Y, Yang X, Mo Y, Fan C, Xiong F, Ren D, Ye X, Li C, Wang Y, Wei F, Guo C, Wu X, Li X, Li Y, Li G, Zeng Z, Xiong W. Circular RNAs function as ceRNAs to regulate and control human cancer progression. MOL CANCER 2018; 17.
18. Zang J, Lu D, Xu A. The interaction of circRNAs and RNA binding proteins: An important part of circRNA maintenance and function. J NEUROSCI RES 2020; 98:87-97.
19. Jiang C, Xu D, You Z, Xu K, Tian W. Dysregulated circRNAs and ceRNA network in esophageal squamous cell carcinoma. Front Biosci (Landmark Ed) 2019; 24:277-90.
20. Xin L, Liu L, Liu C, Zhou LQ, Zhou Q, Yuan YW, Li SH, Zhang HT. DNA-methylation-mediated silencing of miR-7-5p promotes gastric cancer stem cell invasion via increasing Smo and Hes1. J CELL PHYSIOL 2020; 235:2643-54.
21. Xu Y, Yao Y, Gao P, Cui Y. Upregulated circular RNA circ_0030235 predicts unfavorable prognosis in pancreatic ductal adenocarcinoma and facilitates cell progression by sponging miR-1253 and miR-1294. Biochem Biophys Res Commun 2019; 509:138-42.
22. Pan M, Li M, You C, Zhao F, Guo M, Xu H, Li L, Wang L, Dou J. Inhibition of breast cancer growth via miR-7 suppressing ALDH1A3 activity concomitant with decreasing breast cancer stem cell subpopulation. J CELL PHYSIOL 2020; 235:1405-16.
23. Qiu L, Huang Y, Li Z, Dong X, Chen G, Xu H, Zeng Y, Cai Z, Liu X, Liu J. Circular RNA profiling identifies circADAMTS13 as a miR-484 sponge which suppresses cell proliferation in hepatocellular carcinoma. MOL ONCOL 2019; 13:441-55.
24. Guo JN, Li J, Zhu CL, Feng WT, Shao JX, Wan L, Huang MD, He JD. Comprehensive profile of differentially expressed circular RNAs reveals that hsa_circ_0000069 is upregulated and promotes cell proliferation, migration, and invasion in colorectal cancer. Onco Targets Ther 2016; 9:7451-8.
25. Panda AC. Circular RNAs Act as miRNA Sponges. ADV EXP MED BIOL 2018; 1087:67-79.
26. Jian X, He H, Zhu J, Zhang Q, Zheng Z, Liang X, Chen L, Yang M, Peng K, Zhang Z, Liu T, Ye Y, Jiao H, Wang S, Zhou W, Ding Y, Li T. Hsa_circ_001680 affects the proliferation and migration of CRC and mediates its chemoresistance by regulating BMI1 through miR-340. MOL CANCER 2020; 19:20.
27. Alam KJ, Mo JS, Han SH, Park WC, Kim HS, Yun KJ, Chae SC. MicroRNA 375 regulates proliferation and migration of colon cancer cells by suppressing the CTGF-EGFR signaling pathway. INT J CANCER 2017; 141:1614-29.
28. Park SY, Lee CJ, Choi JH, Kim JH, Kim JW, Kim JY, Nam JS. The JAK2/STAT3/CCND2 Axis promotes colorectal Cancer stem cell persistence and radioresistance. J Exp Clin Cancer Res 2019; 38:399.
29. Decker T, Schneller F, Hipp S, Miething C, Jahn T, Duyster J, Peschel C. Cell cycle progression of chronic lymphocytic leukemia cells is controlled by cyclin D2, cyclin D3, cyclin-dependent kinase (cdk) 4 and the cdk inhibitor p27. LEUKEMIA 2002; 16:327-34.

30. Park SY, Lee CJ, Choi JH, Kim JH, Kim JW, Kim JY, Nam JS. The JAK2/STAT3/CCND2 Axis promotes colorectal Cancer stem cell persistence and radioresistance. J Exp Clin Cancer Res 2019; 38:399.
31. Li WC, Wu YQ, Gao B, Wang CY, Zhang JJ. MiRNA-574-3p inhibits cell progression by directly targeting CCND2 in colorectal cancer. Biosci Rep 2019; 39.
32. Nielsen J, Christiansen J, Lykke-Andersen J, Johnsen AH, Wewer UM, Nielsen FC. A Family of Insulin-Like Growth Factor II mRNA-Binding Proteins Represses Translation in Late Development. MOL CELL BIOL 1999; 19:1262-70.
33. Lederer M, Bley N, Schleifer C, Huttelmaier S. The role of the oncofetal IGF2 mRNA-binding protein 3 (IGF2BP3) in cancer. SEMIN CANCER BIOL 2014; 29:3-12.
34. Jonson L, Christiansen J, Hansen T, Vikesa J, Yamamoto Y, Nielsen FC. IMP3 RNP safe houses prevent miRNA-directed HMGA2 mRNA decay in cancer and development. CELL REP 2014; 7:539-51.
35. Ennajdaoui H, Howard JM, Sterne-Weiler T, Jahanbani F, Coyne DJ, Uren PJ, Dargyte M, Katzman S, Draper JM, Wallace A, Cazarez O, Burns SC, Qiao M, Hinck L, Smith AD, Toloue MM, Blencowe BJ, Penalva LO, Sanford JR. IGF2BP3 Modulates the Interaction of Invasion-Associated Transcripts with RISC. CELL REP 2016; 15:1876-83.

Table

Table 1 Relationship between has_circ_0000231 and CCND2 expression and clinicopathological data

clinicopathological features		expression of hsa_circ_0000231		P value	expression of CCND2		P value
		Low	High		Low	High	
Gender				0.791			0.262
	Male	44	39		48	43	
	Female	36	41		32	37	
Age at diagnosis				0.162			0.715
	≤ 60	19	27		21	19	
	＞60	61	53		59	61	
Tumor size (cm)				**0.032***			0.260
	≤ 5	18	8		14	9	
	＞5	62	72		66	71	
Location				0.733			0.391
	proximal	26	24		22	27	
	distal	54	56		58	53	
Differentiation				0.750			0.078
	Well-moderate	44	46		41	52	
	Poor	36	34		39	28	
Depth of invasion				0.122			**0.032***
	T1-T2	13	21		8	18	
	T3-T4	67	59		72	62	
Lymph node metastasis				**0.002***			0.514
	No	7	22		11	14	
	Yes	73	58		69	66	
TNM stage				**0.015***			**0.043***
	I-II	9	21		16	7	
	III-IV	71	59		64	73	
distant metastasis				0.276			0.514
	No	65	70		69	66	

	Yes	15	10		11	14

Figures

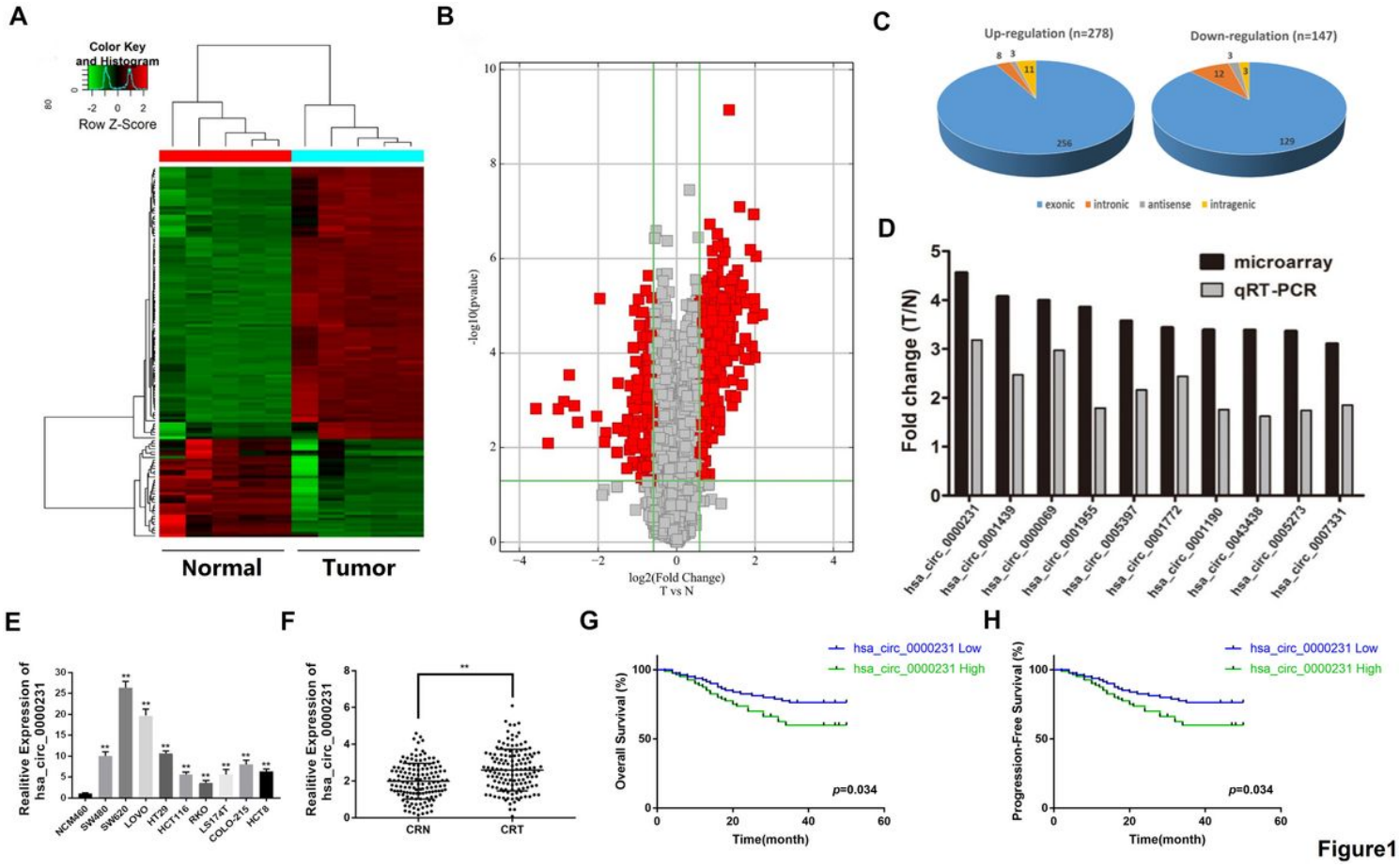

Figure 1

Expression profiles of circRNA and the correlation between has_circ_0000231 and poor prognosis of CRC A. The cluster heat maps displayed the increased and decreased circRNAs. Each column indicates a sample while each row indicates an individual circRNA. The red and green strips represent high and low expression, respectively. B. The volcano plot visualizes the expression of circRNA between CRC tissues and adjacent. C. Classification of differentially expressed circRNA between CRC tissues and adjacent. D. qRT-PCR assay was used to verify the results of circRNA microarray assay. E. Relative expression of has_circ_0000231 in CRC cell lines was determined by qRT-PCR. F. Relative expression of has_circ_0000231 in CRC tissues (CRT) and adjacent normal tissues (CRN) was detected by qRT-PCR (n = 160). G. Kaplan-Meier survival curve of overall survival in 160 patients with CRC according to the hsa_circ_0000231 expression. Patients were divided into high expression and low expression group by

median expression. H. Kaplan-Meier survival curve of progression-free survival in 160 patients with CRC according to the hsa_circ_0000231 expression. Patients were divided into high expression and low expression group by median expression.

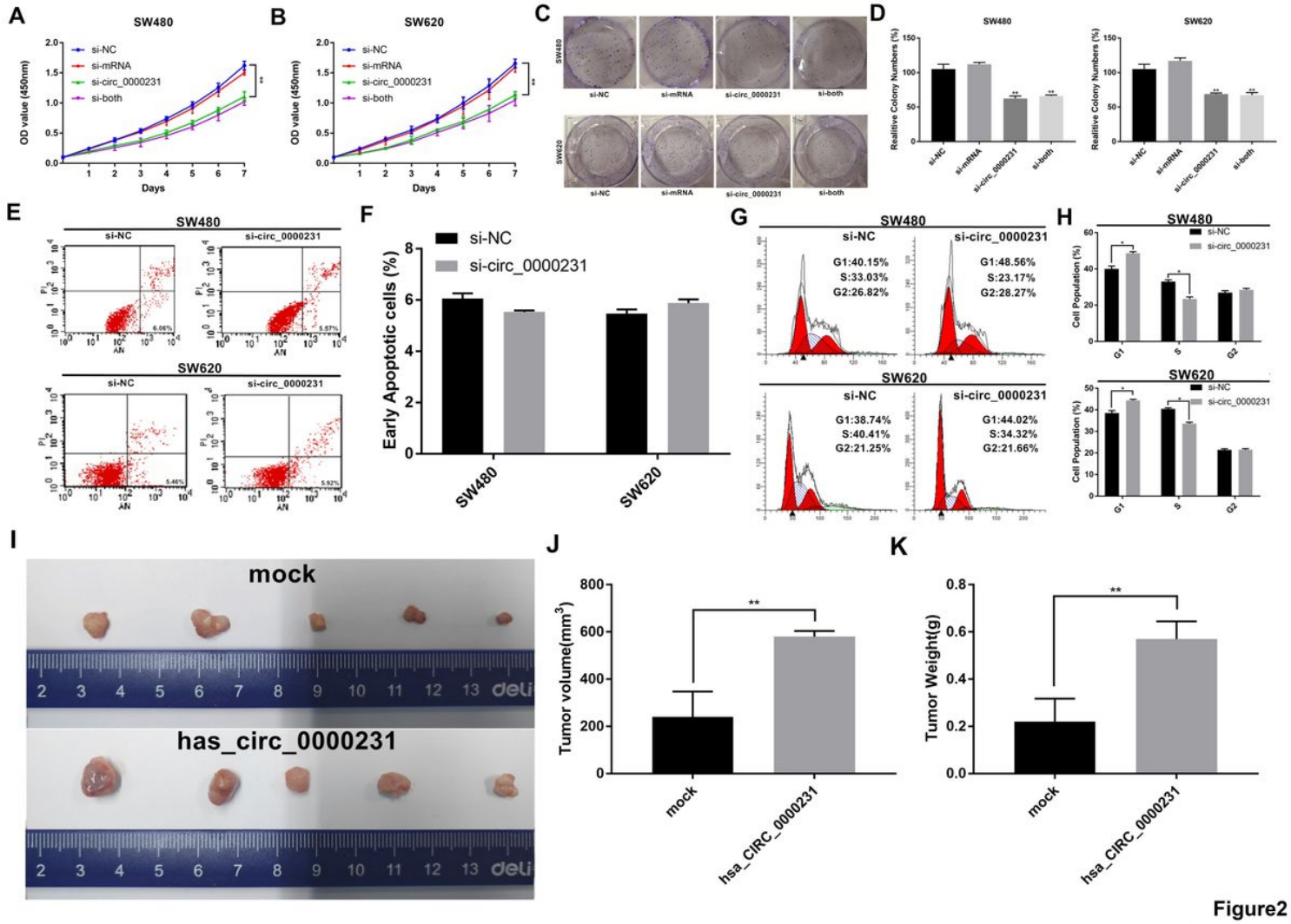

Figure2

Figure 2

hsa_circ_0000231 promotes cell proliferation and tumor growth in vitro and in vivo in CRC A and B. CCK8 assay was performed to detect the effect of hsa_circ_0000231 on cell proliferation. C and D. Colony formation assays were executed to detect the proliferation of cells transfected with indicated vectors. E and F. Apoptosis rate was analyzed by flow cytometry after downregulation of hsa_circ_0000231. G and H. The cell cycle progression was analyzed by flow cytometry after downregulation of hsa_circ_0000231. I. Images of xenograft tumors of each group (n = 5). J. Tumor volume was shown. K. Tumor weight was shown. Data were showed as mean ± SD, *p < 0.05, **p < 0.001.

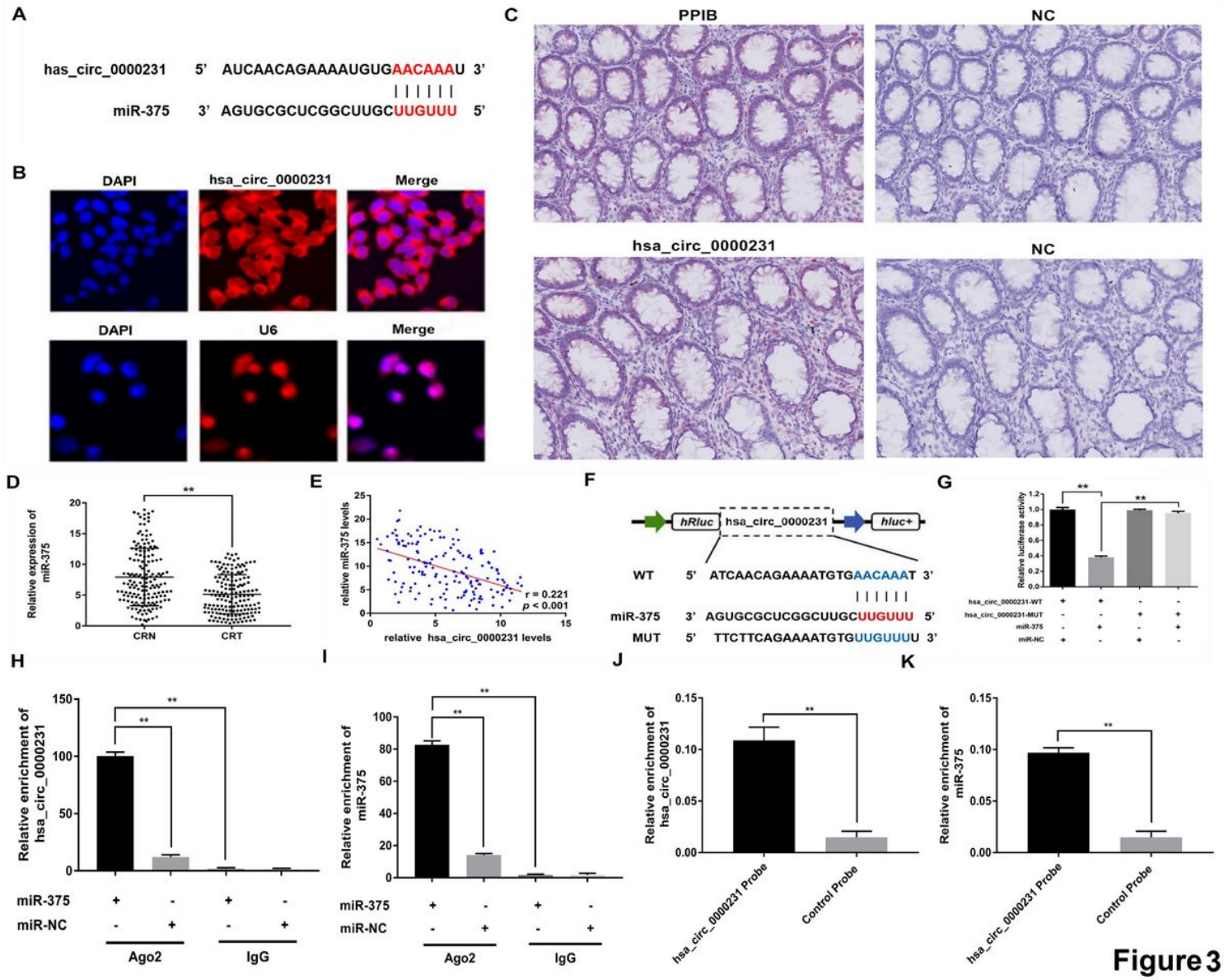

Figure 3

hsa_circ_0000231 functions as a sponge for miR-375 in CRC A. The miR-375 binding site on hsa_circ_0000231 predicted by targetScan and miRanda. B. FISH assay was performed to observe the cellular location of hsa_circ_0000231 (red) in cells (magnification, × 200, scale bar,50 μm) C. BaseScope assay was performed to observe the cellular location of hsa_circ_0000231 (red) in CRC tissues (magnification, × 100, scale bar, 100 μm) D. Relative expression of miR-375 in CRC tissues (Tumor) and adjacent non-tumor tissues (Normal) was tested by qRT-PCR (n = 160). E. Pearson correlation analysis of hsa_circ_0000231 and miR-375 expression in 160 CRC tissues. F. Schematic illustration of hsa_circ_0000231-WT and hsa_circ_0000231-Mut luciferase reporter vectors. G. The relative luciferase activities were detected in SW620 cells after transfection with hsa_circ_0000231-WT or hsa_circ_0000231-Mut and miR-375 mimics or miR-NC, respectively. H and I. Anti-AGO2 RIP was executed in SW620 cells after transfection with miR-375 mimic or miR-NC, followed by western blot and qRT-PCR to detect AGO2 protein, hsa_circ_0000231 and miR-375, respectively. J and K. RNA pull-down was executed

in SW620 cells, followed by qRT-PCR to detect the enrichment of hsa_circ_0000231 and miR-375. Data were showed as mean ± SD, *p < 0.05, **p < 0.001.

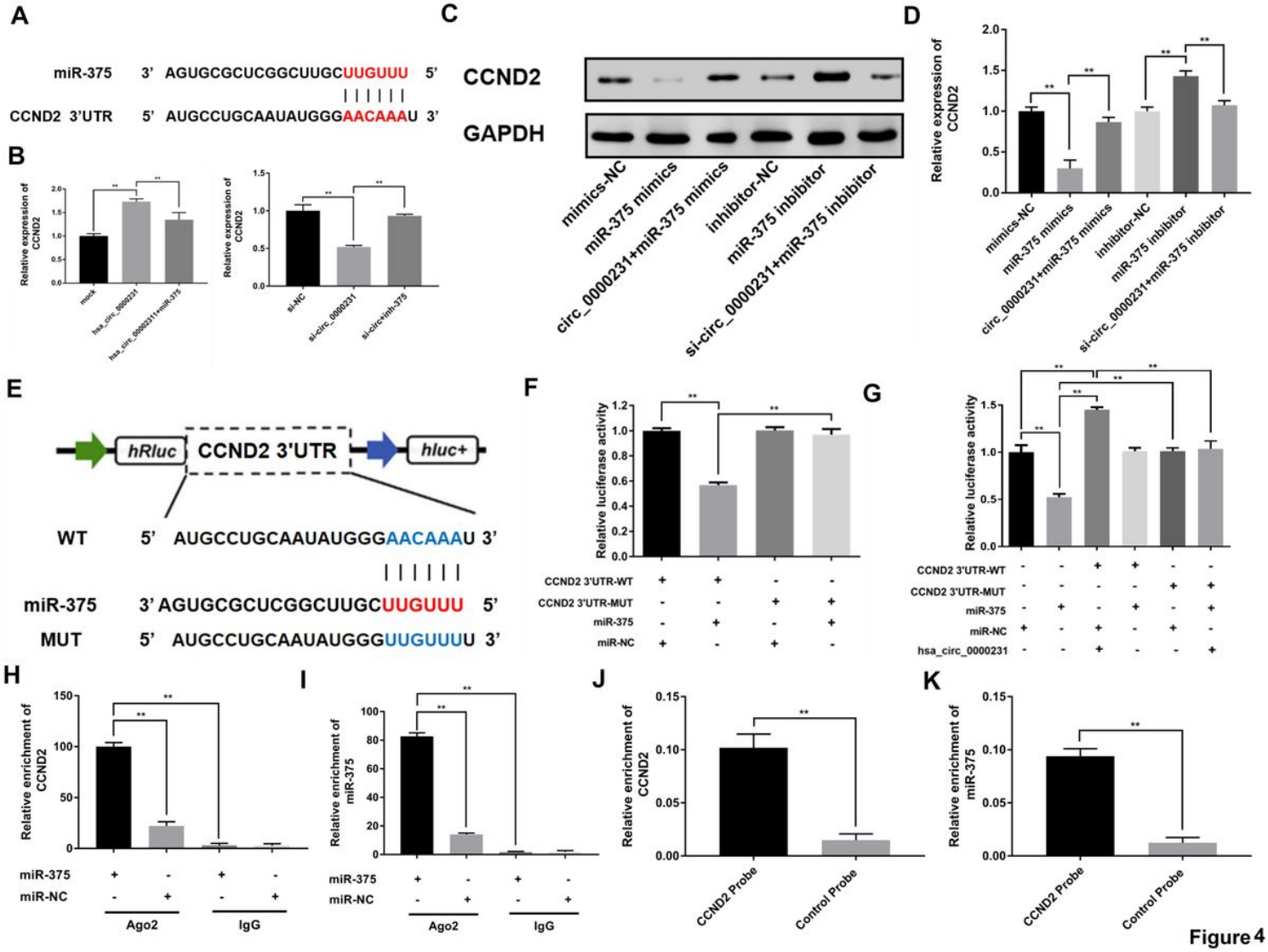

Figure 4

Figure 4

CCND2 is directly targeted by miR-375 and indirectly regulated by hsa_circ_0000231 A. Schematic illustration of CCND2 3'UTR-WT and CCND2 3'UTR-Mut luciferase reporter vectors. B. Relative expression of CCND2 was detected by qRT-PCR in cells transfected with indicated vectors, miRNAs or inhibitors. C and D. Western blot assay was performed to determine the relative expression of CCND2 transfected with indicated vectors, miRNAs or inhibitors. E. Schematic illustration of CCND2 3'UTR-WT and CCND2 3'UTR-Mut luciferase reporter vectors. F. The relative luciferase activities were detected in 293 T cells after transfected with CCND2 3'UTR-WT or CCND2 3'UTR-Mut and miR-375 mimics or miR-NC, respectively. G. Tthe luciferase activity was recovered after transfection with hsa_circ_0000231 in the miR-375 + CCND2 3'UTR-WT group H and I. Anti-AGO2 RIP was executed in SW620 cells after transfection with miR-375 mimic or miR-NC, followed by western blot and qRT-PCR to detect AGO2 protein, hsa_circ_0000231 and miR-375, respectively. J and K. RNA pull-down was executed in SW620 cells, followed by qRT-PCR to

detect the enrichment of hsa_circ_0000231 and miR-375. Data were showed as mean ± SD, *p < 0.05, **p < 0.001.

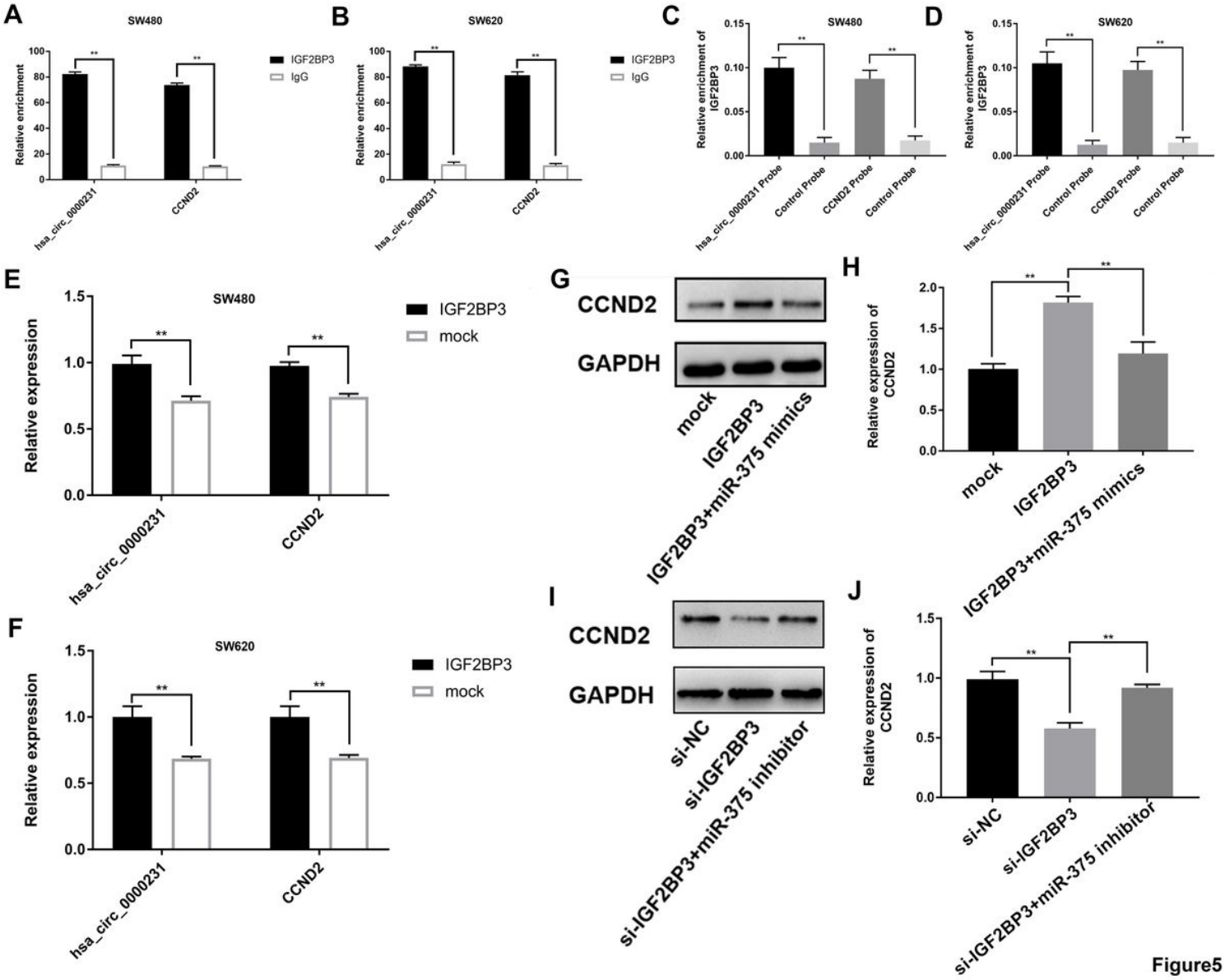

Figure 5

IGF2BP3 could bind to has_circ_0000231 and CCND2, as an RBP to protect the stability of RNA A and B. Anti-IGF2BP3 RIP was executed in SW620 and SW480 cells followed by western blot and qRT-PCR to detect IGF2BP3 protein, hsa_circ_0000231 and CCND2, respectively. C and D. RNA pull-down was executed in SW620 and SW480 cells, followed by qRT-PCR to detect the enrichment of hsa_circ_0000231 and CCND2, respectively. E and F. qRT-PCR was used to detect expression of hsa_circ_0000231 and CCND2 after overexpression of IGF2BP3. G-J. Western Blot assay was conducted to confirm the relative expression of CCND2 transfected with indicated vectors, miRNAs or inhibitors in SW480 cells Data were showed as mean ± SD, *p < 0.05, **p < 0.001.

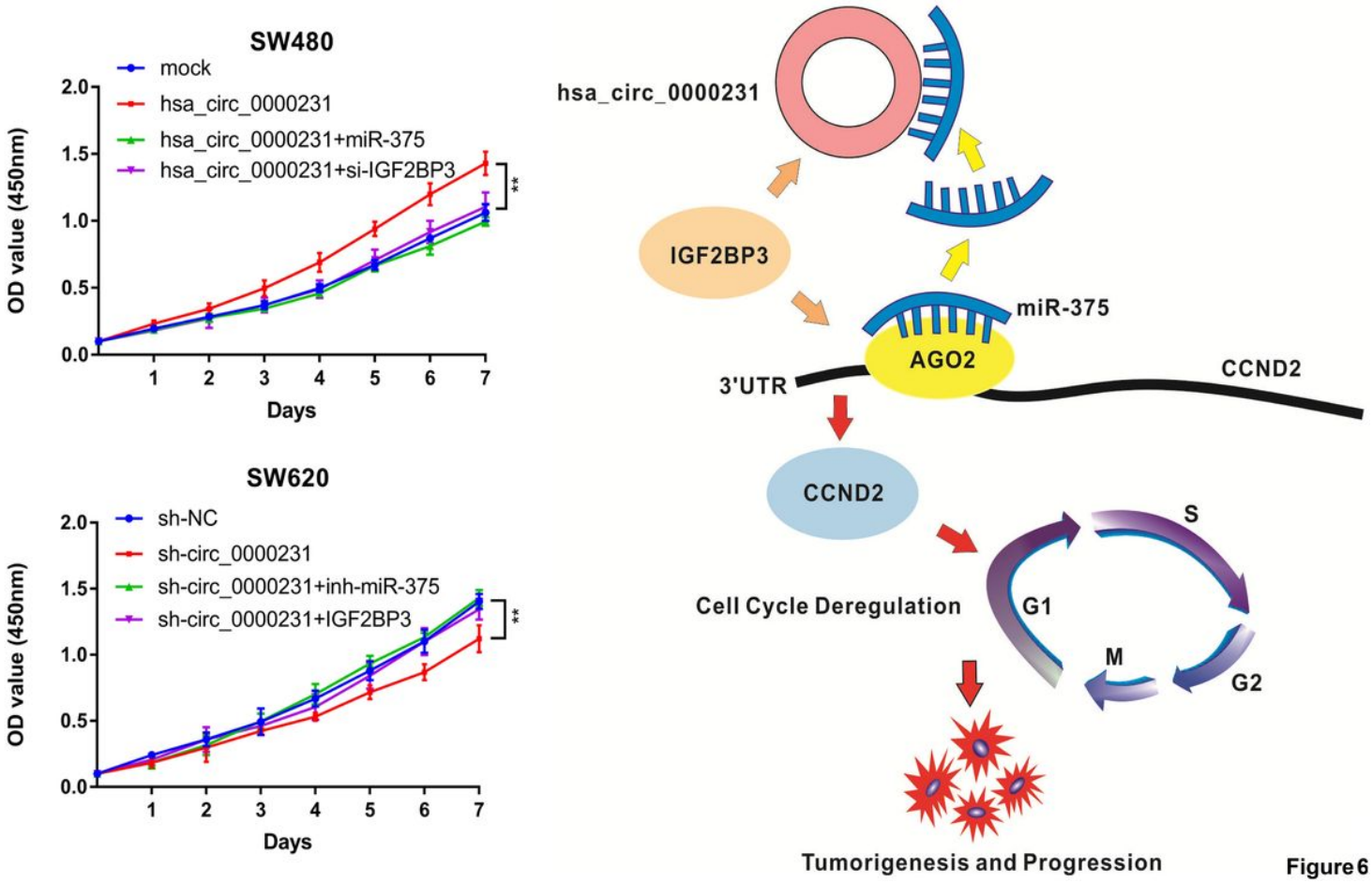

Figure 6

hsa_circ_0000231 promotes CRC proliferation through hsa_circ_0000231/IGF2BP3/miR-375/CCND2 axis A and B. The cell proliferations were determined after transfection with indicated vectors, miRNAs or inhibitors by CCK-8 assays, respectively. C. Schematic diagram of how hsa_circ_0000231 promotes CRC tumorigenesis and progression. D. Data were showed as mean ± SD, *p < 0.05, **p < 0.001.

Supplementary Files

This is a list of supplementary files associated with this preprint. Click to download.

- FigureS2.jpg
- FigureS1.jpg
- TableS5.docx
- TableS4.docx
- TableS3.docx
- TableS2.docx
- TableS1.docx